

Magnetic induction and domain walls in magnetic thin films at remanence

This article has been downloaded from IOPscience. Please scroll down to see the full text article.

2005 J. Phys.: Condens. Matter 17 1711

(<http://iopscience.iop.org/0953-8984/17/10/025>)

View [the table of contents for this issue](#), or go to the [journal homepage](#) for more

Download details:

IP Address: 129.252.86.83

The article was downloaded on 27/05/2010 at 20:26

Please note that [terms and conditions apply](#).

Magnetic induction and domain walls in magnetic thin films at remanence

**Florin Radu^{1,5}, Vincent Leiner¹, Kurt Westerholt¹, Hartmut Zabel¹,
Jeffery McCord², Alexei Vorobiev³, Janos Major³, David Jullien⁴,
Hubert Humblot⁴ and Francis Tasset⁴**

¹ Institut für Experimentalphysik/Festkörperphysik, Ruhr-Universität Bochum,
D-44780 Bochum, Germany

² Leibniz Institute for Solid State and Materials Research Dresden, Helmholtzstrasse 20,
D-01171 Dresden, Germany

³ Max-Planck-Institut für Metallforschung, Heisenbergstraße 3, D-70569 Stuttgart, Germany

⁴ Institut Laue-Langevin, F-38042 Grenoble Cedex 9, France

E-mail: florin.radu@rub.de

Received 9 December 2004, in final form 9 February 2005

Published 25 February 2005

Online at stacks.iop.org/JPhysCM/17/1711

Abstract

Magnetic domain walls in thin films can be well analysed using polarized neutron reflectometry. Well defined streaks in the off-specular spin-flip scattering maps are explained by neutron refraction at perpendicular Néel walls. The position of the streaks depends only on the magnetic induction within the domains, whereas the intensity of the off-specular magnetic scattering depends on the spin-flip probability at the domain walls and on the average size of the magnetic domains. This effect is fundamentally different and has to be clearly distinguished from diffuse scattering originating from the size distribution of magnetic domains. Polarized neutron reflectivity experiments were carried out using a ³He gas spin filter with an analysing power as high as 96% and a neutron transmission of approximately 35%. Furthermore, the off-specular magnetic scattering was enhanced by using neutron resonance and neutron standing wave techniques.

(Some figures in this article are in colour only in the electronic version)

1. Introduction

Magnetic domain imaging at remanence and during magnetization reversal has become an extremely important discipline in the area of magnetic thin films. For magnetoelectronic and spintronic device applications, the domain state and switching behaviour of various vertically

⁵ Author to whom any correspondence should be addressed.

and laterally structured magnetic systems requires detailed investigations in the space and time domain. The experimental techniques available for domain imaging provide either real space information, such as magnetic force microscopy (MFM) [1, 2], Kerr microscopy (KM) [3], Lorentz microscopy (LM) [4–6], polarized electron emission microscopy (PEEM) [7, 8], and secondary-electron microscopy with polarization analysis (SEMPA) [9], or reciprocal space information, such as resonant soft x-ray magnetic small angle scattering (SAS) [10]. In any case, magnetic domain information is obtained via magnetic stray fields emanating from the sample (MFM) or via the local magnetic polarization. Most of the methods currently available do not concentrate on the magnetic domain walls, their thickness, and their orientation.

In this paper we report on the observation of magnetic domain walls, using polarized neutron reflectivity (PNR). PNR has proven in the past to be an essential tool for the analysis of magnetic thin films and heterostructures, including their interfaces and domain structures [11–13]. Here we will go one step further and show that magnetic domain walls can be characterized via pronounced streaks in the off-specular spin-flip (SF) scattering regime. Usually, off-specular SF neutron reflectivity is symmetric ($R_{-+} = R_{+-}$) and is discussed in terms of the Fourier transform of the magnetic domain distribution in the film plane and/or in terms of interfacial magnetic roughness [14–18]. Off-specular asymmetric SF reflectivity ($R_{-+} \neq R_{+-}$) can be observed, if the magnetic induction in the sample and the external magnetic field to the sample are not collinear [19–23]. This leads to SF processes at the sample/vacuum interface, which are always accompanied by a Zeeman energy change of the neutrons. Consequently, the SF neutrons follow a different path in the external applied field (off-specular) to the non-spin-flip (NSF) neutrons (specular). The effect we report here has to be clearly distinguished from either one of these cases. We observe a striking new and asymmetric off-specular neutron reflectivity in the remanent state of a Co film, which is bunched into pronounced streaks. We argue that the asymmetry is caused by breaking the translational symmetry for the neutrons travelling in the film plane, when crossing domain walls with different magnetic potentials on either side of the wall. Neutron scattering at Bloch walls in bulk ferromagnets has been reported in the literature [26–30]. In the present work, we consider neutron scattering from domain walls in thin films with an incident angle to the domain walls close to normal. Analysis of the characteristic features of the off-specular SF scattering reveals the magnetic induction of the film at remanence, the average domain wall width, the average domain size, and the domain wall angle.

Since neutron scattering at domain walls is weak, enhancement factors have been employed, using neutron standing wave properties below the critical angle of total reflection, and neutron resonance conditions above the critical angle. A detailed theoretical background and description of the experimental conditions necessary for realizing either Bright–Wigner resonances or neutron standing waves in thin magnetic films is provided in [31]. Furthermore, the method requires a full spin analysis of the off-specular spin-flip intensity over a large solid angle. This has been achieved with a supermirror in the incident beam and a ^3He spin filter in the exit beam. The polarized gas was provided by TYREX third-generation ^3He filling station recently commissioned at ILL [32].

2. Experimental results

For the present experiment we used a 250 nm thick Co film, grown by rf sputtering on a SiO_2 substrate. Due to exposure to air, a 2.5 nm thick oxide layer is formed on top of the Co layer. The growth conditions and substrate choice provided a polycrystalline Co film.

The magnetization reversal was characterized by the magneto-optical Kerr effect (MOKE) and by wide field Kerr microscopy in the longitudinal mode. MOKE hysteresis measurements

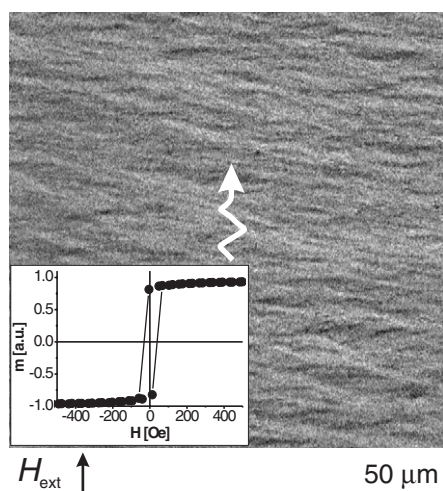


Figure 1. Ripple-like domain structure after applying a saturation field of $H_{\text{ext}} = 2000$ Oe and returning to close to the remanent state at $H_{\text{ext}} = 10$ Oe. The mean magnetization direction together with the ripple-like domain structure is indicated by the curly arrow. The inset shows the hysteresis loop measured by means of the MOKE.

did not reveal any macroscopic anisotropy within the film plane. A characteristic Kerr domain image is shown in figure 1, taken after saturating the sample at +2000 Oe and reducing the field to 10 Oe.⁶ A strongly modulated low angle domain structure can be recognized, which is due to the polycrystalline nature of the film combined with the intrinsic magnetocrystalline anisotropy of Co. The magnetization within the ripple domains is partly tilted to the left and to the right, and is essentially perpendicular to the applied magnetic field (spin-flop orientation). The ripple can be recognized also in the hysteresis loop shown in the inset of figure 1, where a reduced remanence is observed. The magnetization direction within the domains increasingly deviates from the mean magnetization direction when approaching the coercive field, where the reversal of magnetization proceeds by domain wall motion. At remanence, the deviation of the local magnetization vector from the mean direction can also be recognized from the hysteresis loop shown in the inset of figure 1.

We have carried out the neutron reflectivity measurements using the ADAM and EVA reflectometers at the Institut Laue-Langevin, Grenoble, EU. The EVA reflectometer is used in combination with a wide angle ^3He spin-filter analyser. The half-life time of the spin filter was 180 h and the analysing power of the filter was 96%, at the beginning of the experiment, which is comparable to the best performance of a supermirror analyser. The neutron measurements were carried out at 300 K and for two magnetic states of the sample: saturation (not shown here) and remanence. First the sample was saturated, then the field was reduced to zero field (termed *pristine state*). The pristine state is shown in figure 2.

The diagonal intensity ridges stretching from the lower left to the upper right corner are the specular NSF R++ and R-- reflectivities. The specular ridge is rich in features, confirming standing waves and Kiessig fringes in the R++ map above the critical edge for total reflection at the Co film, and standing wave features in the R-- map below the critical edge of the substrate. The situation is dramatically different for the spin-flip (SF) maps R+- and R-+. Aside from the specular ridges, there is additional off-specular intensity following

⁶ This field close to remanence was chosen to be comparable to the guiding field during PNR measurements.

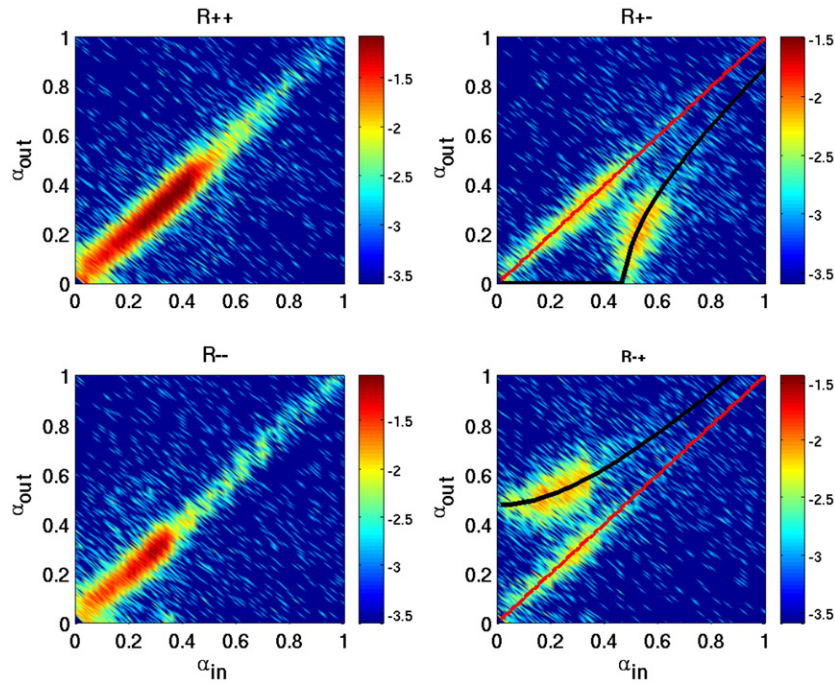


Figure 2. The left column shows intensity maps for the non-spin-flip cross sections R++ (top) and R-- (bottom), the right column for the spin-flip cross sections R+- (top) and R+ (bottom). The maps were recorded close to remanence (≈ 10 Oe). The intensities are plotted in terms of exit angles (y -axis) versus incident angle (x -axis). The streaks are due to reflection and refraction from perpendicular magnetic domain walls, as described in more detail in the text. The black curves are calculated off-specular spin-flip streaks.

a well defined curvature. In the R+- map the additional line of intensity appears at lower exit angles than the specular beam, while in the R+ map this line is located at higher exit angles than the specular beam. Moreover, both off-specular intensity lines exhibit a banana shaped curvature, which, in addition, is intensity modulated in a fashion similar to the specular spin-flip reflectivity. These two features can be explained qualitatively and quantitatively as being due to domain wall scattering.

3. Discussion

First we would like to discuss the key elements which define the intensity of spin-flip scattering at domain walls (DW). For one large domain wall D_{DW} , the neutron will adiabatically follow the magnetic induction and no SF scattering occurs. In contrast, for very small D_{DW} the spin-flip probability is very small. Therefore, the thickness of the domain wall affects the scattered off-specular intensity. Second, the transmitted intensity through the DW is affected by the angle γ between the magnetization vectors in neighbouring magnetic domains. For $\gamma = 0$ no SF scattering is expected; for $\gamma = 90^\circ$ the SF scattering should have a maximum. Also, for $\gamma = 180^\circ$ one should observe off-specular scattering because, even though the neutron spins do not flip, the magnetic field flips instead, leading to a non-SF (with respect to the incident neutron polarization) off-specular signal. Third, the number of domain walls that the neutron passes through before being reflected or transmitted by the next interface affects the

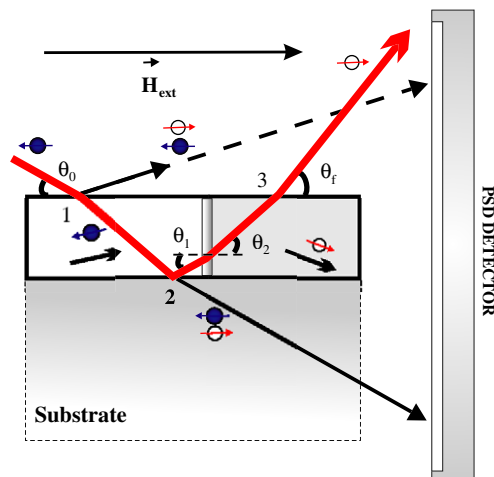


Figure 3. Schematic outline of the polarized neutron path in a magnetic film containing domain walls. The thin (red) arrows indicate neutrons oriented parallel to the magnetic field induction inside and outside of the magnetic film, while thin (blue) arrows indicate neutrons oriented antiparallel to the magnetic field induction. The thick (red) lines show the $(-+)$ neutron path before and after entering the film, which contains two magnetic domains, separated by a perpendicular magnetic domain wall. The magnetization within domains is lying in the sample plane. In this graph it is assumed that spin flip occurs only once, at the domain wall where the neutron enters the grey shade magnetic domain. At the lower interface the neutron is reflected. At the domain wall between the white and grey domain, refraction occurs with spin flip. The neutron leaves the top interface without spin flip. Notice that in general the neutron beam will meet a variable number of domain walls, depending on the incidence angle. This will affect the off-specular intensity but not the position of the streaks.

off-specular intensity. This gives information about the average lateral size of the magnetic domains. Numerical calculations of the transmission coefficient as a function of D_{DW} show that for SF scattering at domain walls a finite DW width and an angle $\gamma > 0$ are required.

The type of the domain wall, Bloch versus Néel, can be inferred from the splitting of the neutron resonances. It was shown that stray fields emerging from the sample as reported in [24] cause a splitting of the resonant angles for the different polarizations [25]. Assuming that Bloch walls give rise to stray fields, and Néel walls do not, then through the stray fields one can discriminate between these two types of domain walls. For the present case we have seen no splitting of the neutron resonances (data not shown). Therefore, we suggest that at least partial Néel walls are present in the sample.

Next we discuss the banana shaped curvature of the off-specular SF scattering. Imagine that down polarized neutrons ($(-)$ polarized opposite to the field direction) enter into a magnetic domain as schematically indicated in figure 3. We assume that the magnetic induction vector in the domain is tilted with respect to the polarization direction of the incident neutrons as shown in figures 1 and 3. Let us follow the path (red line) of the neutrons, which are off-specularly scattered into the $(-+)$ channel. The $(-)$ neutrons will meet the vacuum/sample interface at position No 1 and will then be transmitted without spin flip into the layer⁷. Their quantization axis will turn parallel to the magnetic induction inside of the magnetic domain (\mathbf{B}_{D1}) (white). Travelling further, deep into the layer, they will be reflected at the bottom interface without spin flip. After reflection, they will cross a perpendicular (to the surface plane) magnetic

⁷ A fraction of neutrons will be specularly reflected back into the air, and another fraction will be spin flipped.

domain wall (No 2) and enter into the next magnetic domain (grey shade). The orientation of the magnetic induction inside of this domain (\mathbf{B}_{D2}) is tilted away from the magnetic induction (\mathbf{B}_{D1}) in the previous domain by a tilt angle γ .

Now we make a basic and fundamental assumption, which is essential for the interpretation of the banana shaped off-specular intensity. We assume that the neutrons, which cross a perpendicular domain wall, are being spin flipped and reflected off-specularly. The spin-flip cross section depends on the tilt angle γ . Due to the Zeeman energy change, the SF neutrons will be refracted and they will follow a different path with respect to the NSF neutrons⁸. Next, these neutrons will meet the interface at position No 3 and will exit into the air at an angle $\theta_f^{\text{DW-SF}}$. The same qualitative process also applies for neutrons transmitted through the substrate or for (+) neutrons entering the sample from the top (not shown here).

The qualitative discussion about the neutron paths in the magnetic layer can be cast into a set of equations for the reflection and refraction effects, using Snell's law for neutron optics at each interface, Nos 1, 2, and 3, as indicated in figure 3, yielding the following system of equations:

$$\begin{aligned} k_0^\pm \cos(\theta_0) &= k_1^\pm \cos(\theta_1^\pm) \\ k_1^\pm \sin(\theta_1^\pm) &= k_2^\pm \sin(\theta_2^\pm) \\ k_2^\pm \cos(\theta_2^\pm) &= k_0^\pm \cos(\theta_f^\pm), \end{aligned} \quad (1)$$

where $k_i^\pm = \sqrt{k_0^2 - (u \pm |\mu| |B_D|)}$ are the proper values of the wavevector in the magnetic domains, and θ_i^\pm are the angles of the (+) and (−) neutrons, respectively, as shown in figure 3. The solutions of this system of equations are

$$\begin{aligned} \cos(\theta_f^{\text{DW-NSF}}) &= \cos(\theta_0) \\ \cos(\theta_f^{\text{DW-SF}}) &= \sqrt{\frac{\pm 2\mu B_D}{(\frac{\hbar^2}{2m} k_0^2)} + \cos^2(\theta_0)}, \end{aligned} \quad (2)$$

where $\theta_f^{\text{DW-NSF}}$ and $\theta_f^{\text{DW-SF}}$ are the exit angles of the neutrons with and without spin flip upon crossing the domain wall, respectively, and $k_0 = 2\pi/\lambda$ is the incident wavenumber. The formulae above describe very well all geometric features related to the banana shaped off-specularly reflected neutrons as observed experimentally. For example, the (+−) off-specular SF intensity appears only when the incident angle satisfies the condition $\cos^2(\theta_0) \geq 2\mu B_D / (\frac{\hbar^2}{2m} k_0^2)$, while for the (−+) curve there is no limiting incident angle: the equation $\cos^2(\theta_0) \geq -2\mu B_D / (\frac{\hbar^2}{2m} k_0^2)$ is always satisfied. This is the case for (−) neutrons incident on Co, which has a negative scattering length density. The streaks can be reproduced by the following set of values (shown by black solid curves in figure 2): $|\mathbf{B}_{D1}| = |\mathbf{B}_{D2}| = 15\,500$ G, $\gamma = 30^\circ$, and perpendicular domain walls. $|\mathbf{B}_{D1,2}|$ is reduced compared to the measured saturation value of 17 200 G, which we believe is due to spin canting within the domains. Furthermore, the intensity of the streaks contains additional information, from which the average domain wall width [27], the average domain size $D_D \approx 14\,000$ nm, and the distribution of domain wall angles can be determined. A full quantitative account of all features observed in the maps and also a discussion of other magnetic materials, which have a positive potential barrier for both incident neutron states, is provided elsewhere [31].

In passing we stress that the discussion of the off-specular and asymmetric streaks in terms of optical paths taken by neutrons inside the sample is equivalent to geometrical optics of electromagnetic waves, which explains the propagation of wavefields. Clearly, a complete

⁸ Certainly, a fraction of neutrons will not be spin flipped. In this case there is no Zeeman energy change and thus there will be no deviation from their specular path direction.

analysis using the distorted wave approximation should explain both the geometry and the intensity [16]. There, however, the refraction at the domain walls is not accounted for. The present analysis has the advantage of providing a clear and lucid geometric interpretation with quantifiable parameters of the magnetic induction in the Co film even at remanence.

4. Conclusions

In summary, we have measured with polarized neutron reflectivity the specular and off-specular magnetic scattering from a ferromagnetic Co film in the remanent magnetic domain state. We have analysed the off-specular magnetic neutron scattering using a ^3He gas spin filter. The off-specular spin-flip scattering is dominated by streaks above and below the specular ridge. They appear due to spin-flip transmission at domain walls. These streaks at well defined angles are clearly to be distinguished from magnetic diffuse scattering centred symmetrically at the specular ridge, the latter being due to the size distribution of magnetic domains. In the former case we were able to show that the streaks can be explained by refraction and reflection of spin-polarized neutrons at perpendicular domain walls. We suggest that this is a new method for determining the magnetization $M(T, H = 0)$ in thin films with domains.

Acknowledgments

We would like to thank V K Ignatovich for valuable suggestions and a critical reading of the manuscript, and Andrew Wildes and Boris Toperverg for valuable discussions. This work was supported by Sonderforschungsbereiche 491 'Magnetische Heteroschichten: Struktur und elektronischer Transport' of the Deutsche Forschungsgemeinschaft. The neutron scattering experiments were performed at the ADAM (BMBF grant No 03ZA6BC1) and EVA (of Max Planck Institute, Stuttgart [33]) reflectometers at the Institut Laue-Langevin, Grenoble, EU.

References

- [1] Rugar D and Hansma P 1990 *Phys. Today* **43** 23
- [2] Hartmann U 1999 *Annu. Rev. Mater. Sci.* **29** 53
- [3] McCord J, Schafer R, Mattheis R and Barholz K U 2003 *J. Appl. Phys.* **93** 5491
- [4] Zweck J, Zimmermann T and Schuhrke T 1997 *Ultramicroscopy* **67** 153
- [5] Kirk K J, Chapman J N and Wilkinson C D W 1999 *J. Appl. Phys.* **85** 5237
- [6] Brückner W *et al* 2004 *J. Magn. Magn. Mater.* **283** 82
- [7] Fischer P *et al* 1998 *J. Phys. D: Appl. Phys.* **31** 649
- [8] Kuch W 2003 *Appl. Phys. A* **76** 665
- [9] Scheinfein M R *et al* 1990 *Rev. Sci. Instrum.* **61** 2501
- [10] Kortright J B *et al* 2001 *Phys. Rev. B* **64** 092401
- [11] Fitzsimmons M R *et al* 2004 *J. Magn. Magn. Mater.* **271** 103
- [12] Ankner J F and Zabel H 2003 *Mater. Res. Soc. Bull.* **28** 918
- [13] Radu F, Eitzkorn M, Siebrecht R, Schmitte T, Westerholt K and Zabel H 2003 *Phys. Rev. B* **67** 134409
- [14] Felcher G P and te Velthuis S G E 2001 *Appl. Surf. Sci.* **182** 209
- [15] Langridge S, Schmalian J, Marrows C H, Dekadjevi D T and Hickey B J 2000 *Phys. Rev. Lett.* **85** 4964
- [16] Toperverg B P, Rühm A, Donner W and Dosch H 2001 *Physica B* **297** 160
- [17] Lee W-T, te Velthuis S G E, Felcher G P, Klose F, Gredig T and Dahlberg E D 2002 *Phys. Rev. B* **65** 224417
- [18] Theis-Bröhl K, Schmitte T, Leiner V, Zabel H, Rott K, Brückl H and McCord J 2003 *Phys. Rev. B* **67** 184415
- [19] Ignatovich V K 1978 *Pis. JETP* **28** 311
- [20] Felcher G P, Adenwalla S, De Haan V O and Van Well A A 1995 *Nature* **377** 409
- [21] Korneev D A, Bodnarchuk V I and Ignatovich V K 1996 *J. Phys. Soc. Japan* **65** (Suppl. A) 37
- [22] Fredrikze H, Rekveldt T, vanWell A, Nikitenko Yu V and Syromyatnikov V 1998 *Physica B* **248** 157

-
- [23] van de Kruijs R W E, Fredrikze H, Rekveldt M Th, van Well A A, Nikitenko Yu V and Syromyatnikov V G 2000 *Physica B* **283** 189
 - [24] Welp U, te Velthuis S G E, Felcher G P, Gredig T and Dahlberg E D 2003 *J. Appl. Phys.* **93** 7726
 - [25] Radu F, Vorobiev A, Major J, Humblot H, Westerholt K and Zabel H 2003 *Physica B* **335** 63
 - [26] Schärpf O 1978 *J. Appl. Crystallogr.* **11** 626
Schärpf O 1978 *J. Appl. Crystallogr.* **11** 631
 - [27] Schärpf O and Strothmann H 1988 *Phys. Scr.* T **24** 58
 - [28] Strothmann H and Schärpf O 1989 *Phys. Scr.* **40** 252
 - [29] Podurets K M and Shilstein S S 2001 *Physica B* **297** 263
 - [30] Peters J and Treimer W 2001 *Phys. Rev. B* **64** 214415
 - [31] Radu F *et al* 2005 unpublished
 - [32] Tasset F, Andersen K, Chung R, Humblot H, Jullien D and Regnault L P 2002 *ILL Annual Report* p 106
 - [33] <http://www.ill.fr/YellowBook/EVA/>